Metastable structures of immiscible Fe_xCu_{100-x} system induced by mechanical alloying

1997 J. Phys.: Condens. Matter 9 11077

(http://iopscience.iop.org/0953-8984/9/50/012)

J. Phys.: Condens. Matter **9** (1997) 11077–11083. Printed in the UK PII: S0953-8984(97)86253-4

Metastable structures of immiscible Fe_xCu_{100-x} system induced by mechanical alloying

Shiqiang Wei†‡§, Hiroyuki Oyanagi‡, Cuie Wen‡, Yuanzheng Yang† and Wenhan Liu†

† Center for Fundamental Physics, and Hefei Synchrotron Radiation Laboratory, University of Science and Technology of China, Hefei, 230026, People's Republic of China
‡ Electrotechnical Laboratory, 1-1-4 Umezono, Tsukuba, Ibaraki 305, Japan

Received 23 July 1997

Abstract. The immiscible Fe_xCu_{100-x} alloys have been investigated by x-ray absorption fine structure (XAFS) and transmission electron microscopy (TEM). The TEM results show that the smaller size nanocrystalline particles are obtained by milling for 160 h for Fe–Cu alloys with higher Cu concentration ($Fe_{60}Cu_{40}$). The XAFS results indicate that the local structure of Fe atoms in $Fe_{60}Cu_{40}$ gradually changes from a bcc structure to a fcc one while the Cu atoms maintain the original coordination geometry. In contrast, the local structures around both Fe and Cu atoms in $Fe_{80}Cu_{20}$ alloys which have a larger average grain size indicated a bcc structure after 160 h milling. This suggests that in a mechanical alloying process the grain size strongly affects the alloying limit in the immiscible region. Possible mechanisms of bcc-to-fcc change in $Fe_{60}Cu_{40}$ are discussed in relation to the interdiffusion and the internal pressure effect as a result of small grain size.

1. Introduction

Since the work of Benjamin [1], mechanical alloying (MA) has attracted much attention from viewpoints of applications in magnetooptic thin films and industrial powder metallurgy [2, 3]. Moreover, it has been found that MA can form amorphous alloys in a wide composition range starting at binary or ternary crystalline metal powder mixtures using the solid-state reaction [4, 5], so that one can obtain new amorphous materials with unique physical properties.

Recently, a new interest has arisen due to the discovery that the MA can make some immiscible metals to form the metastable phases which is never obtained by normal metallurgic and quenching method, i.e. Fe–Cu, Cu–Ta, Cu–V, Cu–Ag, Cu–W binary metals [6–9]. This phenomenon seems to indicate that the solid solubility of these immiscible binary metals can be greatly extended by MA. The mechanically alloyed Fe_xCu_{100-x} solid solution is a representative system, its solid solubility and structure have been widely investigated by Uenishi *et al* [10], Yavari *et al* [11], Crespo *et al* [12, 13] and us [14–16] with differential scanning calorimetry (DSC), x-ray diffraction (XRD), transmission electron microscopy (TEM) and Mossbauer spectroscopy techniques. The DSC results have confirmed that there is a new phase in mechanically alloyed Fe_xCu_{100-x} solid solution, since it showed the exothermic peak in the 550–700 K region. The XRD patterns show the distinct peaks of

§ E-mail address: sqwei@etl.go.jp

0953-8984/97/5011077+07$19.50

fcc copper and bcc iron for initial $Fe_{60}Cu_{40}$ mixture. The bcc α-Fe gradually decreases with the milling time increase. Furthermore, the bcc α-Fe peaks fully disappear after milling for 160 h and only fcc peaks are observed. The bcc α-Fe peaks subsequently return after annealing at 773 K. However, the local structural parameters of Fe and Cu atoms are not yet clear for the mechanically alloyed Fe_xCu_{100-x} solid solutions: whether or not the Fe atoms in the bcc lattice are randomly substituted by Cu atoms after a long-time milling. In more recent studies, we found that the $Fe_{60}Cu_{40}$ supersaturated solid solution still keeps the crystalline structure with a medium-range order by extended x-ray absorption fine structure (EXAFS) and Mossbauer spectroscopy [15, 16]. Three characteristic structures were observed for the $Fe_{60}Cu_{40}$(160 h) solid solution, i.e. the bcc α-Fe, fcc Fe-rich and fcc Cu-rich regions.

In this paper, we aim to study the local structure around Fe and Cu atoms: to clarify the effect of the ball milling and investigate whether immiscible Fe and Cu atoms form a uniformly supersaturated solid solution alloy or not for $Fe_{60}Cu_{40}$(160 h) and $Fe_{80}Cu_{20}$(160 h). TEM was used to measure the shape and particle size distribution of Fe_xCu_{100-x} solid solutions. XAFS has been performed to measure the local structures of Fe and Cu atoms in $Fe_{60}Cu_{40}$ and $Fe_{80}Cu_{20}$ after various degrees of ball milling. Although x-ray and neutron diffraction techniques cannot distinguish the local structures of Fe and Cu atoms, XAFS can characterize the local structures of Fe and Cu sites.

2. Experiment

Crystalline iron and copper powders with purity higher than 99.9% and with particle sizes less than 200 mesh were mixed to the desired composition. The mixture and tungsten carbide balls were sealed inside a cylindrical stainless steel vial filled with argon gas. The weight ratio of the ball to powder is 10:1. MA was performed in a planetary ball with a rotation speed of about 210 rpm. The samples were obtained while Fe_xCu_{100-x} mixtures were milled for 10, 40 and 160 h, they were represented as Fe_xCu_{100-x}(10 h), Fe_xCu_{100-x}(40 h), Fe_xCu_{100-x}(160 h), respectively. Their XRD patterns are reported elsewhere [15]. The mechanically alloyed Fe_xCu_{100-x}(160 h) samples were then examined in a Hitachi H-800 transmission electron microscope operated at 200 kV.

The Fe and Cu K-edge x-ray absorption spectra were measured at the XAFS station of 4W1B beamline of Beijing Synchrotron Radiation Facility. The electron beam energy was 2.2 GeV and the maximum stored current was 50 mA. Data were collected with a fixed exit monochromator using flat Si(111) crystals. The energy resolution was about 2 eV by the Cu foil 3d near K-edge feature. The x-ray harmonics were minimized by detuning the two flat Si(111) crystal monochromator to about 70% of the maximum incident light intensity. Data were collected in a transmission mode using ion chambers with mixed Ar/N_2 fill gas at room temperature. In order to estimate the experimental deviations, the Fe and Cu K-edge absorption spectra of $Fe_{60}Cu_{40}$(160 h), Fe powder and Cu powder were measured three times, respectively. The results show that the deviation is smaller than 1% for the XAFS oscillation signal.

3. Results

The TEM images of $Fe_{80}Cu_{20}$(160 h) and $Fe_{60}Cu_{40}$(160 h) are shown in figure 1. It can be observed that the particles are sphere-shaped and nearly uniform in size. Their average sizes are 350 and 150 Å for $Fe_{80}Cu_{20}$(160 h) and $Fe_{60}Cu_{40}$(160 h), respectively. The result

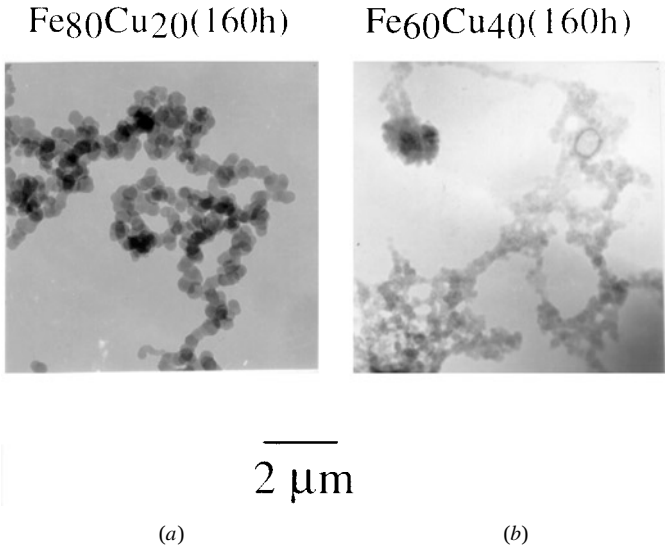

Figure 1. TEM images of (*a*) $Fe_{80}Cu_{20}$(160 h), (*b*) $Fe_{60}Cu_{40}$(160 h).

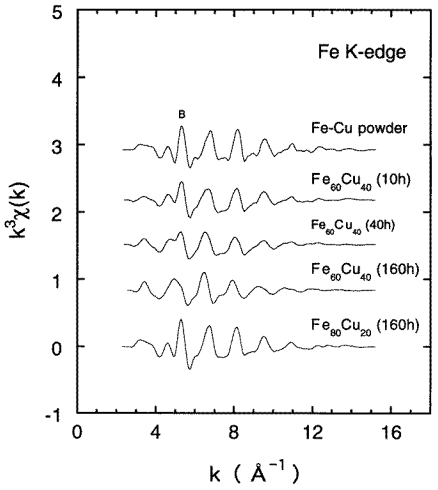

Figure 2. $\chi(k)k^3$ versus k for Fe K-edge of mechanically alloyed Fe_xCu_{100-x}.

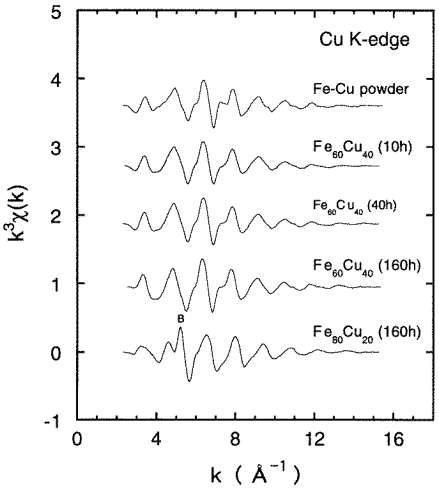

Figure 3. $\chi(k)k^3$ versus k for Cu K-edge of mechanically alloyed Fe_xCu_{100-x}.

indicates that the Fe–Cu mixtures with a higher Cu concentration can make fine particles after a ball milling process. Smaller particles are expected to have large surface area which enhances the Fe–Cu interdiffusion.

Figures 2 and 3 demonstrate the EXAFS function $\chi(k)k^3$ of mechanically alloyed Fe_xCu_{100-x} solid solutions. A sharp peak B at $k = 5.22$ Å^{-1} in the $\chi(k)k^3$ of bcc α-Fe powder is characteristic of a bcc structure. This feature gradually decreases for $Fe_{60}Cu_{40}$ solid solutions with the milling time, and fully disappears when the milling time reaches 160 h. This feature is observed in the Cu EXAFS function $\chi(k)k^3$ of $Fe_{80}Cu_{20}$(160 h). The results indicate that the local structure of Fe atoms in $Fe_{60}Cu_{40}$ gradually transforms from a bcc-like coordination to a fcc-like one as the MA process proceeds. Second, for starting

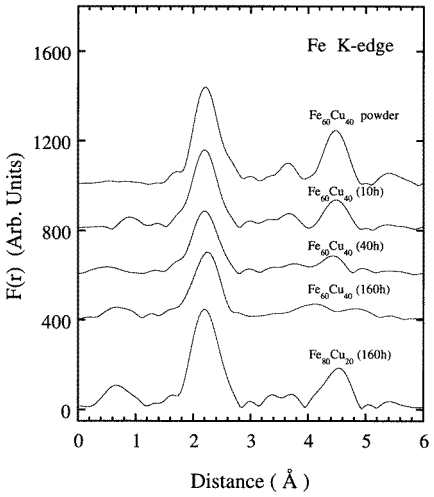

Figure 4. The FT of Fe for mechanically alloyed Fe_xCu_{100-x}.

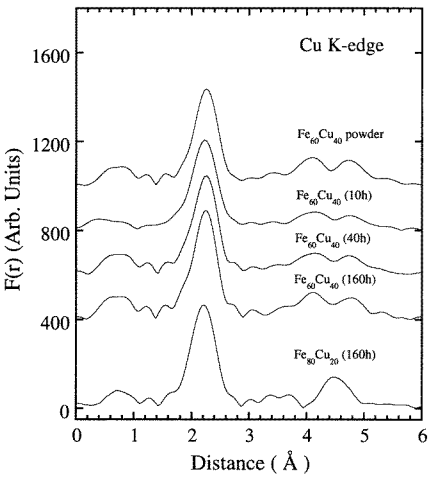

Figure 5. The FT of Cu for mechanically alloyed Fe_xCu_{100-x}.

Fe–Cu mixtures with high Fe concentration, the same milling process (160 h) gives rise to the bcc-like local structure for both Fe and Cu atoms, which is consistent with these results observed with XRD [15, 17].

The Fourier transform (FT) of the Fe K-EXAFS oscillations $\chi(k)k^3$ for mechanically alloyed Fe–Cu solid solutions are shown in figure 4. A strong peak around 2.2 Å indicates the first nearest-neighbour atoms. The magnitude intensity of the third peak ($R = 4.48$ Å) which is sensitive to the coordination geometry is not observed in the FT for $Fe_{60}Cu_{40}$(160 h). It is clear that the FT of the Fe K-EXAFS for $Fe_{60}Cu_{40}$(160 h) become similar to that of Cu K-EXAFS for metal Cu in figure 5. The FT of Fe K-EXAFS for $Fe_{60}Cu_{40}$(160 h) shows that MA changes the local structure of Fe atoms from a bcc-like structure to a fcc-like one. The magnitude of the first peak decreases on the milling proceeds, for example the magnitude drops about one third after milling for 160 h. The FT result of Fe K-EXAFS for $Fe_{80}Cu_{20}$(160 h) suggests that the local structure of Fe atoms remains to be a bcc-like structure after 160 h milling. The magnitude intensity of the first peak is the same as that of its initial Fe–Cu powder mixture, indicating that MA does not increase the disorder parameter. Using the amplitude $|F(k, \pi)|$ and phase shift $\phi(k)$ of standard samples obtained from the bcc α-Fe and fcc metal Cu, i.e. $Fe_{60}Cu_{40}$ powder mixture, the curve fitting was performed [18]. The results are summarized in tables 1 and 2.

4. Discussion

The MA mechanism is a complicated process and difficult to be described with a simple model. It has been observed that the resultant products usually consist of nanocrystalline and amorphous phases after MA [2]. For the solid state amorphization of binary or ternary systems with a large negative heat of mixing, it is also difficult to interpret the alloying mechanism in the MA process. However, the mechanism can be attributed to two microscopic origins. One is that the mixed powders are characterized by highly strained small particles with various defects [19]. The other is that one element was fast diffused into the host matrix due to the strong negative heat of mixing [20]. Eckert *et al* [21] reported

Table 1. The structural parameters of Fe_xCu_{100-x} solid solutions fitting for Fe K-edge EXAFS spectra.

	First shell					Second shell				
Sample	Bond type	R (Å)	σ (Å)	N	ΔE_0	Bond type	R (Å)	σ (Å)	N	ΔE_0
Fe–Cu powder	Fe–Fe	2.48		8.0		Fe–Fe	2.86		6.0	
$Fe_{60}Cu_{40}$(10 h)	Fe–M[a]	2.48	0.084	7.8	−1.0	Fe–M	2.84	0.085	3.4	4.5
$Fe_{60}Cu_{40}$(40 h)	Fe–M	2.50	0.094	9.1	1.5	Fe–M	2.83	0.095	2.0	2.6
$Fe_{60}Cu_{40}$(160 h)	Fe–M	2.56	0.092	11.5	1.0					
$Fe_{80}Cu_{20}$(160 h)	Fe–M	2.49	0.079	8.0	2.0	Fe–M	2.85	0.082	5.5	3.8

[a] (M = Fe, Cu).

Table 2. The structural parameters of Fe_xCu_{100-x} solid solutions fitting for Cu K-edge EXAFS spectra.

	First shell					Second shell				
Sample	Bond type	R (Å)	σ (Å)	N	ΔE_0	Bond type	R (Å)	σ (Å)	N	ΔE_0
Fe–Cu powder	Cu–Cu	2.56		12.0						
$Fe_{60}Cu_{40}$(10 h)	Cu–M	2.55	0.089	11.6	2.2					
$Fe_{60}Cu_{40}$(40 h)	Cu–M	2.55	0.090	11.9	2.2					
$Fe_{60}Cu_{40}$(160 h)	Cu–M	2.56	0.089	11.8	4.0					
$Fe_{80}Cu_{20}$(160 h)	Cu–M	2.50	0.079	8.1	2.0	Cu–M	2.84	0.083	5.5	3.8

that the small negative heat of mixing in the Co–Cr, Co–Mn, Ni–Cr, Ni–Mn systems is not sufficient for the formation of an amorphous phase via interdiffusion, but the solid solution can be formed after MA milling.

Although the immiscible systems with positive heat of mixing have not been considered as promising means of alloy formation from thermodynamical viewpoints [22], Sakurai *et al* [9] found that MA can form the normally immiscible $Cu_{30}Ta_{70}$ amorphous alloys with positive heat of mixing. Their EXAFS results showed, however, that there are amorphous features in the FT for $Cu_{30}Ta_{70}$ sample with 50 h milling, because the magnitude intensity of the main peak is about 10 times lower than that of their crystalline metal Cu and Ta.

In the early-stage studies of immiscible Fe_xCu_{100-x} systems [14], we reported that the structures of mechanically alloyed Fe_xCu_{100-x} solid solutions depend on the mixed powder composition. The Fe_xCu_{100-x} alloys is a single fcc structure for $x < 60$, a mixed fcc and bcc structure for $60 < x < 80$, and a single bcc structure for $x > 80$. Although many research works have studied on the MA Fe_xCu_{100-x} solid solutions [10–16, 23, 24], it is not clear whether the supersaturated $Fe_{60}Cu_{40}$ solid solution is a homogeneous alloy or not.

In order to study the local structural change of Fe_xCu_{100-x} solid solution during the MA process, two special compositions $Fe_{60}Cu_{40}$ and $Fe_{80}Cu_{20}$ were selected for investigation. The EXAFS results show that the radial distribution functions of Fe_xCu_{100-x} solid solutions are different from those of the mechanically alloyed Ni–Mo and Cu–Ta systems which have amorphous features [5, 9]. The Fe_xCu_{100-x} solid solutions still preserve the polycrystalline structure after 160 h of milling. Therefore, the MA can drive the Fe_xCu_{100-x} solid solutions into nanometre grains but it does not greatly destroy their crystalline structure. Furthermore, we find that the higher Cu atomic concentration in the original Fe–Cu mixture results in a smaller grain size after milling. When the Cu atomic concentration is decreased from 40 to 20%, the average grain sizes are significantly increased from 150 to 350 Å.

For $Fe_{80}Cu_{20}$(160 h), the EXAFS results in figures 4 and 5 demonstrate that the bcc-structure is maintained for Fe atoms but the fcc-structure Cu atoms changes into a bcc-like one after milling. The structural parameters in table 1 illustrate that the bond distance ($R_{Cu-M} = 2.50$ Å) and coordination number ($N = 8.1$) are 0.06 Å shorter and 4 smaller than those of the metal Cu, respectively. The results indicate that the Cu atoms are incorporated into the bcc α-Fe phase for $Fe_{80}Cu_{20}$(160 h) by MA. The reason why the Fe local structure of $Fe_{80}Cu_{20}$(160 h) does not change into a fcc one is possibly related to the fact that the lower Cu ratio (20% Cu) results in a larger particle size, but the higher Cu ratio (40% Cu) can form a smaller particle size.

For $Fe_{60}Cu_{40}$, it was found that the magnitude of the main peak in the FT of Cu K-EXAFS does not show a noticeable change with the milling time while the main peak intensity for the Fe K-EXAFS decreases by $\frac{1}{3}$. This suggests that the local structure around Cu atoms in $Fe_{60}Cu_{40}$(160 h) does not change by MA but the local structure of Fe atoms is seriously modified. Two different interpretations are postulated. In the first case, Fe atoms are incorporated into the fcc-lattice of Cu because of large surface area in $Fe_{60}Cu_{40}$(160 h) as shown in figure 1. In the second interpretation, the bcc-lattice of Fe undergoes a first-order phase transition from a bcc-like coordination to a fcc-like dense packing as the internal pressure surpasses a critical pressure. In the former case, the Fe–Cu alloying is achieved while in the latter case, they form the separated Fe and Cu clusters. If all Fe atoms were incorporated into a fcc Cu lattice, the Cu lattice is expected to have a large distortion which would appear as a sharp drop of the Cu main FT peak intensity. Since we find that the Cu local structure is not changed during the MA, the former case is unlikely.

From viewpoints of interface diffusion, the Cu atoms near the Fe grain boundary are easier in alloying into a fcc phase. From viewpoints of internal pressure or stress, a smaller grain size is advantageous for phase change. Doyama *et al* [25] and Keavney *et al* [26] reported that 11 layers of fcc-phase Fe could be epitaxially grown on the Cu(001) and Cu_xAu_{1-x} single crystal. It was confirmed that the small size Fe cluster can stably exist. In $Fe_{80}Cu_{20}$(160 h) where Fe particles do not form small size clusters, both Cu and Fe atoms have bcc-like medium-range order. In $Fe_{60}Cu_{40}$(160 h), the local structure of Fe atoms gradually transits to a fcc structure from a bcc one as the particle size become very small.

Summarizing the results, for the mechanically alloyed Fe_xCu_{100-x} solid solution, it is likely that the resultant products are mixed by small-size Fe and Cu clusters. The internal core of Fe and Cu clusters may be pure elements and the alloying region is only in the coherent interface of both Fe and Cu clusters. This conclusion is supported by the results of Mossbauer spectroscopy [16] where the Fe-rich and Cu-rich were reported, and high-resolution TEM [27] where it can be observed the clear particle boundary and the particle sizes are about 20–30 Å.

5. Conclusion

With the XAFS and TEM techniques, we have obtained the quantitative structural parameters of Fe and Cu nearest-neighbour coordination for $Fe_{60}Cu_{40}$ and $Fe_{80}Cu_{20}$ solid solutions. The EXAFS results revealed that the mechanically alloyed Fe_xCu_{100-x} is an inhomogeneous solid solution depending on the initial composition. For the higher Cu concentrations in Fe–Cu mixtures, the MA resulted in small clusters. We found that the local structure of Fe atoms in $Fe_{60}Cu_{40}$ gradually changes from a bcc structure to a fcc-like one as the MA process proceeds, while the Cu atoms still maintain the original coordination geometry. It is likely that the resultant particles in $Fe_{60}Cu_{40}$(160 h) consist of mixed small-size Fe and Cu clusters in which Cu atoms can be dissolved only at the coherent boundary.

Acknowledgments

We would like to thank Dr Tiandou Hu for his help in performing the XAFS experiment and also thank Beijing Synchrotron Radiation Facility for giving us the beam time for the XAFS measurement. This work was supported by the National Natural Science Foundation of China and President Foundation of Chinese Academy.

References

[1] Benjamin J S 1970 *Metall. Trans.* **1** 2943
[2] Schultz L 1988 *Mater. Sci. Eng.* **97** 15
[3] Koch C C, Cavin O B, Mckamey G G and Scarbrough J O 1983 *Appl. Phys. Lett.* **43** 1017
[4] Eckert J, Schultz L and Urban K 1990 *J. Less-Common Met.* **166** 293
[5] Cocco G, Enzo S, Barrett N T and Roberts Z J 1992 *Phys. Rev.* B **45** 7066
[6] Shingu P H, Ishihara K N, Uenishi K, Kuyama T, Huang B and Nasu S 1990 *Solid State Powder Proceeding* (The Minerals Metals and Materials Society) p 20
[7] Fukunaga T, Mori M, Inou K and Mitzutani U 1991 *Mater. Sci. Eng.* A **134** 863
[8] Gaffet E, Louison C, Harmelin M and Faudet F 1991 *Mater. Sci. Eng.* A **134** 1380
[9] Sakurai K, Yamada Y, Ito M, Lee C H, Fukunaga T and Mizutani U 1990 *Appl. Phys. Lett.* **57** 2660
[10] Uenishi K, Kobayashi F, Nash S, Hatano H, Ishihara K N and Shingu P H 1992 *Z. Met.* **83** 132
[11] Yavari A R, Desre P J and Benameur T 1992 *Phys. Rev. Lett.* **68** 2235
[12] Crespo P, Hernando A, Yavari R, Drbohlav D, Escorial A G, Barandiaran J M and Orue I 1993 *Phys. Rev.* B **48** 7134
[13] Crespo P, Hernando A and Escorial A G 1994 *Phys. Rev.* B **49** 13 227
[14] Yang Y Z and Dong Yuanda 1992 *Acta Metall. Sin.* **28** 399
[15] Wei S Q, Yin S L, Liu W H, Liu F X, Gao C, Yang Y Z, Dong Y D and Hu T D 1994 *J. Phys. Sin.* **43** 1630
[16] Li T, Li Y Z, Zhang Y H, Gao C, Wei S Q and Liu W H 1995 *Phys. Rev.* B **52** 1120
[17] Huang J Y, He A Q, Wu Y K, Ye H Q and Li D X 1996 *J. Mater. Sci.* **31** 4165
[18] Sayers D E and Bunker B A 1988 *X-ray Absorption, Principles, Applications, Techniques of EXAFS, SEXAFS and XANES* ed D C Koningsberger and R Prins (New York: Wiley) p 211
[19] Ermakov A E, Yivichikov E E and Barinov V A 1981 *Fiz. Met. Metalloved.* **52** 1184
[20] Dubois J M 1988 *J. Less-Common Met.* **145** 309
[21] Eckert J, Schultz L and Urban K 1988 *J. Less-Common Met.* **145** 283
Eckert J, Schultz L and Urban K 1990 *J. Less-Common Met.* **166** 293
[22] Miedema A R, De Chatel P F and De Boer F R 1980 *Physica* **100B** 1
[23] Schilling P J, He J-H, Cheng J and Ma E 1996 *Appl. Phys. Lett.* **68** 767
[24] Huang J Y, Yu Y D, Wu Y K, Ye H Q and Dong Z F 1996 *J. Mater. Res.* **11** 2717
[25] Doyama M, Matsui M, Matsuoka H, Mitani S and Doi K 1991 *J. Magn. Magn. Mater.* **93** 374
[26] Keavney D J, Storm D F, Freeland J W, Grigorov I L and Walker J C 1995 *Phys. Rev. Lett.* **74** 4531
[27] Huang J Y, Wu Y K, He A Q, Hu K Y and Meng Q M 1994 *J. Chin. Electron Microsc. Soc.* **13** 26